Scholars' Mine

Spring 2017

The viability of ADVANTG deterministic method for synthetic radiography generation

Andrew Albert Bingham

THE VIABILITY OF ADVANTG DETERMINISTIC METHOD FOR SYNTHETIC

RADIOGRAPHY GENERATION

by

ANDREW ALBERT BINGHAM

A THESIS

Presented to the Graduate Faculty of the

MISSOURI UNIVERSITY OF SCIENCE AND TECHNOLOGY

In Partial Fulfillment of the Requirements for the Degree

MASTER OF SCIENCE

in

NUCLEAR ENGINEERING

2017

Approved by

Dr. Hyoung K. Lee, Advisor
Dr. Ayodeji B. Alajo
Dr. Xin Liu

ABSTRACT

Time sensitive and high resolution image simulations are needed for synthetic ra-
diography generation. The standard stochastic approach requires lengthy run times with
poor statistics at higher resolutions. The investigation of the viability of a deterministic
approach to synthetic radiography image generation was explored. The aim was to analyze
a computational time decrease over the stochastic method. ADVANTG was compared to
MCNP in multiple scenarios including a Benchtop CT prototype, to simulate high resolu-
tion radiography images. By using ADVANTG deterministic code to simulate radiography
images the computational time was found to decrease over 10 times compared to the MCNP
stochastic approach.

ACKNOWLEDGMENTS

Thank you to Dr. Hyoung K. Lee for advising me and directing my research and sitting through every single presentation. Thank you to my committee members. I also want to thank those two special graduate students who helped me throughout the research process and made it that much more enjoyable (you know who you are). I want to thank Abigail Perona for supporting me and walking with me every step of the way on this journey. Finally I want to thank God for the blessings and opportunities to complete this thesis.

TABLE OF CONTENTS

Page

SECTION

LIST OF ILLUSTRATIONS

LIST OF TABLES

1. INTRODUCTION

Complex radiation transport problems have been solved by using transport codes for generations. Of these transport codes MCNP (Monte Carlo N-Particle) has been the most widely accepted transport code because of its proven ability to realistically model radiation transport problems. While many other codes exist such as SCALE or Geant4 (GEometry ANd Tracking) for regulatory processes and for research MCNP is the standard which other codes are measured. As robust as the MCNP transport code is, there are some situations where using MCNP is cumbersome. In modeling radiography images, while MCNP can certainly model a CT (Computed Tomography) system and create synthetic radiographs, the problem lies with the nature of the code. The main concern with the code is the run time of a standard CT simulation. MCNP simulations of CT systems can take days to complete, this is problematic if time sensitive situations call for more immediate results. As such a deterministic approach was researched to decrease the computational time while retaining accuracy. ADVANTG (AutomateD VAriaNce reducTion Generator) is a deterministic transport code based on Denovo (3-D discrete ordinates transport code) Evans [2012], the goal of the research is to generate radiography images from MCNP and ADVANTG and compare the image quality to the computational time required to generate said images. Using MATLAB^{TM} to compare image differences, it should be possible to determine if ADVANTG is a viable approach for decreasing the computational time required to generate radiography images.

1.1. GENERAL RADIOGRAPHY

Computed radiography is defined as the acquisition and storage of x-ray images. Wolbarst [2012] For digital systems a common method uses a flat panel detector with an array of semiconductors to obtain the x-ray signal directly. This has many applications such

as medical or nondestructive imaging. Typically a scintillating material is used to convert the x-ray into light that is then counted. Cesium Iodide(CsI) and gadolinium oxysulfide are the most common scintillators used because of the high resolution yields. The image quality is dependent on a number of factors including; exposure time, current, voltage, and detector to source distance. While using x-rays to image people or objects is beneficial, in some cases, using a physical x-ray system can cause an unnecessary dose. By simulating the radiography image it is possible to reduce the amount of unnecessary exposure as well create an expected result for benchmarking before a real radiography is preformed. Another benefit is time, by using a simulation it is possible to generate an expected result in a short period of time.

1.2. MCNP THEORY

"MCNP is a general-purpose Monte-Carlo N-Particle code that can be used for neutron, photon, electron, ... transport." Team [2003] The code was developed by Los Alamos National Laboratory and was used in the photon only transport mode throughout the research. MCNP simulates individual particle behavior and uses a statistical sampling process based on a random number generator, also referred to as random walk method. MCNP uses particle weights for computational efficiency, weights can be applied to particles to simulate a number of particles emitted from a source. A particle weight is essentially a correction for deviation from the physical transport. Team [2003] Monte Carlo methods primary rely on two base equations to solve the Boltzmann equation; the probability density function Eq.1.1 and the path length Eq.1.2

$$g(F) = f(x)|dx/dF| \qquad (1.1)$$

$$f(x) = e^{-x} \qquad (1.2)$$

Using Eq.1.1 and Eq.1.2 MCNP can simulate particle track lengths from the mean free path and the probability of that interaction using the cumulative probability density function and solve for the flux of the system in $particles/cm^2/s$. Lewis and W.F. Miller [1993] MCNP input file is broken into three main sections, referred to as cards. These cards are cell cards, surface cards, and data cards. The cell and surface cards contain information that describes the geometry and physical properties of the simulated system. The data cards contain material properties, source definitions, and tallies. The cell card is defined by a cell number, material number, material density, surface unions and intersection, and particle importance. Other information can be include such as fill, universe, and volume. The final cell is a void cell which is defined by 0 material and 0 particle importance and terminates particles tracts in that region. The surface card can be defined by either a surface such as a plane or cylinder, or by a macrobody such as a box or parallelepiped. Most of the research used macrobodies in the form of RPP (Rectangular Parallelepiped), the structure consisted of six plane definitions in the form of x minimum, x maximum, y minimum, y maximum, z minimum, and z maximum, where each plane defines the region of the parallelepiped. Data cards are comprised primarily of material information, source information, and tally information. Material information is defined by a material number, followed by an isotope ZAID (Z-A-Identification) number using ENDF/B-VI.8 libraries, and finally followed by the composition of that isotope. In the case of this specific research the source definitions were used to create a localized point source with the desired x-ray energy. The tally information was also supplied in the data card, primarily for this research in the form of FMESH4. While the FIR5 tally exists, ADVANTG was unable to read in that specific tally type from the MCNP input file, so it was not tested.

1.3. ADVANTG THEORY

By MCNP's nature, as the volume of a FMESH cell decreases the fraction of particles contributing to the flux decreases. As such the uncertainty will increase. "Thus Monte Carlo calculations may not be as appropriate as deterministic methods in these cases." Lewis and W.F. Miller [1993] For a simulation that requires less than $50\mu m$ per voxel Monte Carlo methods quickly require more particles and more computational time to have the same flux and error. The focus of the research is to investigate if ADVANTG discrete ordinates solver can produce similar radiography images as MCNP with less computational time. ADVANTG uses three-dimensional discrete ordinates (S_N) transport solution from Denovo. Denovo is a 3-D discrete ordinates transport code from Oak Ridge National Laboratory. The discrete ordinates is a deterministic methods that discretizes the transport equation and solves a linear system of equations through iterations. Mosher et al. [2015] Specifically ADVANTG discretizes the transport problem from a user supplied mesh grid and executes the deterministic code (Denovo) to solve the transport equation. Discrete ordinates rely on quadrature sets which define the angular coordinates required to simulate the direction of photon travel. In case of ADVANTG these two angles are defined as polar and azimuthal angles. Eq.1.3 is the general three-dimensional discrete ordinates equations. Lewis and W.F. Miller [1993]

$$\Omega * \nabla\Psi(\vec{r},\Omega) + \sigma(\vec{r})\Psi(\vec{r},\Omega_n) = q(\vec{r},\Omega_n) \tag{1.3}$$

ADVANTG takes a known flux at the source location by running a first collision Monte-Carlo simulation and then calculates the flux at each voxel boundary. One thing that should be noted are anomalies in the flux distribution called ray effects. Ray effects are nonphysical oscillations in the solution of the flux. This is most commonly seen in localized sources or where the scattering is small. Lewis and W.F. Miller [1993] Specifically for ADVANTG a

source located near or on mesh boundaries resulted in oscillations and ray effects. Properly meshing the volume and placing the source location at the center of the voxel mitigates ray effects. Mosher et al. [2015]

1.3.1. Other Deterministic Codes. From literature reviews other deterministic methods were in use or development, namely DORT (Two-Dimensional Discrete Ordinates Transport Code) Rhoades and Childs [1987], TORT (Three-Dimensional Discrete Ordinates Transport Code) Rhoades and Childs [1990], and ATTILA (A proprietary deterministic code from Varian). Other deterministic transport codes were researched, the issue was primarily the availability. Most codes were either proprietary or where not released for public use. Others such as ATTILA were targeted more towards industrial applications and were proprietary codes that can cost a considerable amount. For the specific application a three dimensional transport code was required, so codes similar to DORT that only preformed 2-D simulations, were not practical. The TORT code, while being a three dimensional transport code, was outdated and was replace by Denovo at Oak Ridge National Laboratory in their SCALE package called Exnihilo Johnson et al. [2015] which is shared by ADVANTG. ADVANTG also had the benefits of sharing the geometry and source specifications directly with the MCNP input file which reduced error and inconsistencies during cross code comparison. Overall ADVANTG was the most stable widely available deterministic code that had a robust method for the type of required simulations.

1.3.2. ADVANTG Input Structure. ADVANTG input file relies on two input files, MCNP5 file and a separate ADVANTG file. The MCNP input file can be created as normal, although some limitations with mesh tallies and source definitions do exist. The ADVANTG input file was broken into lots of parameters that mostly define how the deterministic calculation was performed. During the research a few parameters were looked at; methods, materials, angle and quadrature set, and meshing. The primary methods parameter was set to dx or deterministic only calculations and disregarded any variance reduction parameter generation which used either CADIS (Consistent Adjoint Driven Importance Sampling) or

FW-CADIS (Forward-Weighted CADIS) Mosher et al. [2015]. The materials were imported into ADVANTG from the MCNP input; however the materials still needed to be defined in ADVANTG because separate cross section ENDF/B-VII.0 libraries were used for the deterministic calculations. Only two angular parameters were adjusted during the research. The number of azimuthal angles per octant, and the number of polar angles per octant. These angles were used in the deterministic calculation and correspond to the expected level of detail in the results. That last main parameter was meshing size. The meshing size directly defined the discretization boundaries for the deterministic calculation. This required x, y, and z meshing superimposed onto the geometry. The y and z meshing directly represented the resolution of the system in terms of pixels.

2. METHODS

2.1. PROGRAMS AND SETUP

Various computer limitations resulted in multiple computer upgrades throughout the research. For a simplistic simulation a single thread 8GB(Gigabytes) Windows 10 computer was sufficient for simulation completion. As the simulations complexity increased the low specification computer was no longer sufficient. The ADVANTG code was heavily RAM (Random Access Memory) dependent and as the voxel meshing amount increased so did the RAM requirement. The lower RAM requirement was given in the ADVANTG manual where $Mesh$ is the number of mesh voxels, N_g is the number of energy groups, N_k is the number of Krylov vectors, L is the scattering expansion order. N_u is step characteristics method for the spatial discretization and is equal to 1. Mosher et al. [2015]

$$Memory = Mesh * (N_g + N_k) * (L + 1)^2 * N_u * 8bytes \qquad (2.1)$$

$$Mesh = xmesh * ymesh * zmesh \qquad (2.2)$$

So for a small mesh of 78*289*363 the lower RAM requirement is expected to be:

$$Memory = 8182746 * (8 + 20) * (3 + 1)^2 * 1 * 8bytes = 29.327GB \qquad (2.3)$$

Not only was the amount of RAM a limiting factor but the OS (Operating System) was as well. ADVANTG was only compiled in single threaded mode in Windows. A bug was found in the code that made the simulations crash at a reasonably large mesh size when run on a single core. As such the OS was changed to Linux Ubuntu 14.04 where ADVANTG could be complied to run in multi threaded mode. The final system was a 12 core, 128GB, Ubuntu 14.04 system. It must be noted that Windows was still required

for certain programs. Secondary programs were used primarily for pre-processing and post-processing. Notepad++v7.3.2 was used for viewing and editing plain text files and also creating input files for MCNP and ADVANTG. Python2.7.10 was used to post-process MCNP output files as well as a requirement for ADVANTG. VisEd was used to view pre-input files for geometry error as well as view the 3-D model. VisIt was used to post-process and view ADVANTG output files. MATLAB^{TM} was used to generate and digitally process raw data to images and profiles. SpekCalc [Poludniowski and Evans, 2007, Poludniowski, 2007, Poludniowski et al., 2009] was used to generate the x-ray spectrum for the CT system in the MCNP input file. Both MCNP 6.1 and ADVANTG 3.0.3 were run using the command line. Plain text input files were created and called through the terminal to run the simulation. For all simulations both MCNP and ADVANTG input files were created. The main parameters adjusted during the simulation process in MCNP were: Object placement in the form of surface and cell cards, material adjustments, point source location, meshing size, and the number of particle histories. For ADVANTG the adjusted parameters included: the number of polar angles (denovo_quad_num_polar), the number of azimuthal angles (denovo_quad_num_azi), and the meshing size (mesh_x, mesh_y, and mesh_z). The output for MCNP was in the form of plain text file labeled as meshtal generated from the FMESH4 tally to simulate pixels. As for ADVANTG a file was generated called fields.silo, the detector information was retrieved by setting the y and z mesh to the pixel amount. Both of the output files were post-processed to gain the detector information in the form of a plain text file. For MCNP python2.7 was used to reshape the meshtal file into an appropriate array and output as a matrix. The ADVANTG file was post-processed through a program called VisIt and then output as a similar matrix. After each output file had been post-processed into plain text files, they were loaded into MATLAB^{TM} to generate images. Radiographs, contour plots, and profiles were generated along with any necessary scaling, rotating, and corrections. Afterwards the images were saved and compared.

2.2. ISOTROPIC POINT SOURCE VERIFICATION

This initial research investigated the accuracy of both MCNP and ADVANTG compared to theoretical calculations. Both the simulations and the calculation was based on a 100keV mono energetic isotropic point source centered on a 10cm x 10cm detector located 19.875cm away. The detector was split into 100x100 mesh points to simulate a pixel array. The major volume was filled with standard temperature and pressure (STP) air, and the detector was Cesium Iodide. Hubbell and Seltzer [2004] ADVANTG was run with default parameters, and MCNP used $1E^{+10}$ particle histories with no variance reduction. The theoretical calculations were solved in MATLAB$^{\text{TM}}$ using the inverse square law (Eq.2.4) at each pixel.

$$I = 1/(4\pi r^2) \tag{2.4}$$

Using the inverse square law calculations from MATLAB$^{\text{TM}}$ both simulations were compared to the theoretical calculation. This simulation was run different times to resolve low bit images generated from ADVANTG and poor statistics in MCNP. The ADVANTG issue was solved by changing a parameter in the post-processing and was not related to the ADVANTG simulation (see Figures 2.1a and 2.1b). For MCNP the number of particle histories were increased from $1E^{+9}$ to $1E^{+10}$ to reduce the statistical error, the effects of particle histories were explored in more detail and can be seen in the results section.

2.3. AREA SOURCE MODEL

After the isotropic point source simulation had been verified the next step was to simulate a more realistic source. A 1mm x 1mm area source was modeled next to represent the focal spot of the Source-Ray, inc. Model SB-160-4k-BW SourceBlock x-ray tube. Sou Again the process was completed for MCNP and ADVANTG. The results for ADVANTG were undesirable and will be described in the results section. The impacts of the area source results led to the simulation of a point source cone beam that followed similar characteristics.

(a) Detector image banding.　　　　　　　　(b) Detector image without banding

Figure 2.1. Comparison of ADVANTG image banding issue resolved using %g in VisIt

2.4. SIMPLE CONE BEAM

After the results of the area source simulation, a collimated cone beam was simulated. A lead collimator was added to properly shape the beam to yield the same shape as the area source. The materials consisted of STP air, lead collimator, and a Gadolinium Oxysulfide (Gd2O2S) detector. Hubbell and Seltzer [2004] The single source implemented an energy spectrum generated by SpekCalc [Poludniowski and Evans, 2007, Poludniowski, 2007, Poludniowski et al., 2009] at 120kVp and was located 55cm from the surface of the detector. The energy spectrum was generated using specifications from the Benchtop CT flat panel detector. Rayence The point source was located off center to yield the desired beam shape. A 2-D CAD drawling of the system can be seen in Figure 2.3. The cone beam was simulated at various pixel densities, with the end result being to replicate 4x4 binning (578x726 resolution) seen in the Rayence CMOS flat panel detector. Some simulated pixel

Figure 2.2. The x-ray spectrum generated by SpekCalc at 120kvp.

densities included 192x242, 289x363, and 578x726. Radiography images and profiles were generated and will be discussed in the results section.

2.5. BENCHTOP CT MODEL

After the cone beam simulations a full scale prototype model was constructed based on Dr. Hyoung K. Lee's Benchtop CT (seen in Appendix A).The model includes the point source cone beam, collimator, and detector from the previous cone beam simulations. The stage was omitted from the simulations because of the negligible contribution to the output image. The materials were identical to the previous cone beam simulation except for the addition of imaging objects. Images were generated from both MCNP and ADVANTG to

Figure 2.3. A 2-D representation of the cone beam geometry.

test the computational time and image quality for the comparison of a simple objects. The energy spectrum as seen in figure 2.2 used the same energy as the cone beam case. The pixel density of 578x729 was used to simulate the effective pixels in 4x4 binning with a pixel size of $198\mu m$.

2.5.1. Flat Field Correction. For digital radiography and in the specific case of a flat panel detector correcting for the beam angle difference across the detector is referred to as flat field correction. The corrected normalized image is given by the following equation, where P_{nc} is the normalized flat field correction image, $< P_{gain}(x, y) - O(x, y) >$ is the average pixel value $O(x, y)$ is the off set value and $P_{gain}(x, y)$ is the gain image Lee et al. [2005]:

$$P_{nc}(x, y) = (< P_{gain}(x, y) - O(x, Y) >)/(P_{gain} - O(x, y_)) * S \qquad (2.5)$$

For the simulations, the equation above were modified slightly in terms of a completely idealistic scenario where P_{input} is the input image, WI is the plain white image, and DI is the dark image.

$$P_{nc}(x, y) = (P_{input} - DI)/(WI - DI) \tag{2.6}$$

Since the simulations were an ideal situation the dark image was equal to zero resulting in:

$$P_{nc}(x, y) = P_{input}/WI \tag{2.7}$$

By using equation 2.7 the flat field image was generated for each simulated radiography image to create a realistic representation of the Benchtop CT. An example of this process and the impacts will be shown in the results section.

2.5.2. Multi Material Imaging. The multi material imaging consisted of three $2cm^3$ blocks consisting of lead, aluminum, and water with densities of $11.350g/cc$, $2.699g/cc$, and $1.000g/cc$ respectively. Hubbell and Seltzer [2004] The blocks were place in a line, and level with the base of the detector. The blocks were separated by $1cm$ and were located $10cm$ away from the front of the detector. The simulations were run in both MCNP and ADVANTG. The output intensities were post-processed. Both simulations where flat field corrected and normalized. In Figure 2.4 is a 3-D CAD model of the system.

2.5.3. Aluminum Step Block Imaging. The aluminum step block imaging consisted of six steps with surface areas of $1cm^2$ per step, the first step started with a thickness of $6mm$ and decreased by $1mm$ ending with a thickness of $1mm$. The aluminum had a density of $2.699g/cc$. Hubbell and Seltzer [2004] The step block was placed level with the base of the detector and was located $10cm$ away from the front of the detector. The simulations were run in both MCNP and ADVANTG, and the output intensities were post-processed. Both simulations where flat field corrected and normalized. In Figure 2.5 is a 3-D CAD model of the system.

Figure 2.4. A 3-D CAD render of the multi material blocks system consisting of lead, aluminum, and water

Figure 2.5. A 3-D CAD render of the aluminum step block system. With each step decreasing by 1mm

2.5.4. ADVANTG Angular Impact. As described earlier, ADVANTG has parameters that can be defined in the input file to modify how the simulation is preformed. The two major parameters that were modified during the research were polar angles and azimuthal angles. From the simulation of the prototype CT system the generated images contained small artifacts in the image. Modifying the amount of angles was investigated to determine the effects that the number of angles had on the output image. Table 2.1 describes the total angles tested related to the amount of polar and azimuthal angles per octant.

2.5.5. MCNP Particle History Impact. During the research increasing statistical error was seen as the pixel density increased in the MCNP FMESH. This was a known fact before the research began because of the nature of the Monte Carlo method. The statistical

Table 2.1. Total angular amounts represented by azimuthal and polar angles in ADVANTG

Azimuthal Angles	Polar Angles	Total Angles
4	4	128
6	6	288
8	8	512
10	10	800
12	12	1152
14	14	1568
16	16	2048
18	16	2304
20	16	2560
22	16	2816
24	16	3072
37	16	4736

error was expected to increase as the FMESH intervals increased. The aim was to get the statistical error of the FMESH to around 2% or less. As such the impact of the particle histories on the radiography image quality was investigated. During the simulations only the amount of particles were changed. The particle histories investigated were $1E^{+4}$, $1E^{+6}$, $1E^{+9}$, $5E^{+9}$, and $1E^{+10}$.

2.6. COMPUTER AIDED DESIGN IMPORTATION

The final point of the research investigated the viability of importing 3-D CAD models into MCNP and ADVANTG. The purpose was to implement complex models for radiography imaging that would otherwise be difficult or time consuming to code by hand. The first step was to investigate whether importing CAD files in MCNP was possible without a proprietary code. As it turned out VisEd had the native capability to import 2-D and 3-D CAD files. The next process was to model the Benchtop CT system, SolidWorks^{TM} was

used to model the Benchtop CT system and the same multi material blocks used in the previous simulations. After that the CAD system was simulated and compared to the hand created files for ADVANTG only.

3. RESULTS

3.1. ISOTROPIC POINT SOURCE VERIFICATION

The first simplistic case was simulated to verify the accuracy of ADVANTG and MCNP codes before continuing on with a more complex system. Radiography images for each simulation were generated to compare. The radiography images generated from the simulations are located in the Figures 3.1a, 3.1b, and 3.1c. The images alone lacked fine details required to make a conclusion as to whether or not the simulations matched the theoretical calculations. Profiles at the center were generated, normalized and plotted to properly view the results. MCNP was shifted upward and normalized to the curve fit to better visualize the shape relative to the theoretical profile. From Figure 3.2 it is clear that in this specific case ADVANTG was closer to the theoretical values than MCNP. The ADVANTG values differed from the theoretical values by about 2% which was within reason. As for the run times the ADVANTG simulation completed in 461.0 seconds (7.6833 minutes) and MCNP running $10E^{+10}$ completed in 618.2 minutes. ADVANTG completed about 80 times quicker than MCNP.

(a) Point source radiography generated from MCNP   (b) Point source radiography generated from ADVANTG   (c) Theoretical calculations based on Beer-Lambert Law

Figure 3.1. Comparison of radiography images generated from MCNP, ADVANTG, and theoretical calculations.

Figure 3.2. MCNP, ADVANTG, and theoretical profiles along the center of the detector.

3.2. AREA SOURCE MODEL

The area source simulations ran as intended in MCNP, however ADVANTG simulations resulted in ray effects and boundary issues. The abnormal result was arose because of how ADVANTG treats area sources. ADVANTG uses an initial MCNP simulation to run a first collision source. The major caveat is that this first collision source can only be run using a single energy spectrum Mosher et al. [2015] which does not correspond the requirements for our system. Also The area source was located across discretization boundaries in ADVANTG which also caused ray and boundary effects. This effect was also seen if point sources were located near or on a boundary. Since the limitations of this method were not practical for the specific system model, a point source cone beam geometry was chosen instead.

(a) MCNP radiography image of a cone beam with a detector resolution of 192x242

(b) MCNP radiography image of a cone beam with a detector resolution of 192x242

Figure 3.4. Comparison of cone beam radiography images in ADVANTG and MCNP for a detector resolution of 192x242

threads the rendezvous of the simulations were turned off until the very end. Despite this, ADVANTG still finished considerably quicker, it may be possible to reduce the ADVANTG run time even further by adjusting the expansion order and other parameters.

Table 3.1. The simulation times for varying mesh sizes in MCNP and ADVANTG

	192x242	289x363	578x726
MCNP	557.2 minutes	563.4 minutes	558.00 minutes
ADVANTG	4.37 minutes	17.13 minutes	43.18 minutes

3.4. BENCHTOP CT MODEL

After the collimated cone beam shape was verified the Benchtop CT prototype simulated the imaging of objects. The radiography images were equivalent to 4x4 binning resolution 578x726 pixels. Flat field correction was implemented for all Benchtop CT images using Equation 2.7, Figure 3.8 is an example of how flat field correction was implemented.

(a) MCNP radiography image of a cone beam with a detector resolution of 289x363

(b) ADVANTG radiography image of a cone beam with a detector resolution of 289x363

Figure 3.5. Comparison of cone beam radiography images in ADVANTG and MCNP for a detector resolution of 289x363

(a) MCNP radiography image of a cone beam with a detector resolution of 578x726

(b) ADVANTG radiography image of a cone beam with a detector resolution of 578x726

Figure 3.6. Comparison of cone beam radiography images in ADVANTG and MCNP for a detector resolution of 578x726

(a) Intensity profiles for 192x242.

(b) Intensity profiles for 289x363.

(c) Intensity profiles for 578x726.

Figure 3.7. Comparison of cone beam radiography images in ADVANTG and MCNP for a detector resolution of 289x363

Figure 3.8. An example of Flat field correction with an aluminum step block simulation

3.4.1. Multi Material Imaging. The multi material simulation was aimed to view the differences in material density. The goal was to take lead, aluminum, and water and image the materials and output a difference in intensities. In the Figures 3.9a and 3.9b are the comparison of the flat field corrected radiography images from ADVANTG and MCNP. Both images were normalized and used a detector resolution of 578x726. The results show a clear distinction between the different materials. As expected the lead absorbed the most x-rays while water absorbed the least with aluminum in the middle. The comparison of the profiles show an interesting relationship between MCNP and ADVANTG, while the overall shape of the profile is consistent the MCNP profile is shifted. This profile shift

(a) MCNP radiography image of lead, aluminum, and water with a detector resolution of 578x726

(b) ADVANTG radiography image of lead, aluminum, and water with a detector resolution of 578x726

Figure 3.9. Comparison of multi material imaging in ADVANTG and MCNP for a detector resolution of 578x726

was due primarily to the increase in error in MCNP as the pixel density increased. The MCNP simulation took 562.3 minutes to complete and ADVANTG took 43.02 minutes. ADVANTG again was shown to generate similar or even better images in about 13 times less amount of time.

3.4.2. Aluminum Step Block Imaging. The aluminum step block simulations served two purpose. the first purpose was to view the differences in material thickness. The second was to view the effects of penumbra. The main goal was investigating how the codes simulated the differences in thickness, with penumbra being an addition. The images were flat field corrected and normalized and used the same resolution of 578x726. Figures 3.11a, 3.11b, and 3.12 compare the radiography images along with the profiles. Both methods produces quality radiography images that had similar profiles. Again it is possible to observe a shift in the MCNP profile due to the lack of particles per pixel as compared to a more coarse meshing. Even though the radiography images were of similar quality the MCNP simulation took 559.8 minutes while the ADVANTG simulation took

Figure 3.10. Intensity profiles of multi material images for MCNP and ADVANTG with a detector resolution of 578x726.

40.13 minutes. Once again ADVANTG was completed in over 13 times more quickly than MCNP. From the Benchtop CT simulations it can be concluded the ADVANTG can simulate radiography images in a fraction of the time.

3.4.3. ADVANTG Angular Impact. During the Benchtop CT simulations the effects of ADVANTG parameters on the system was investigated. The impact of the number of angles per octant was investigated. In Table 2.1 describes the parameters and the contribution to the amount of total angles. Below is a plot of the profiles of the multi material simulations without flat field correction at varying angles. From 3.13 the profile plot clearly shows negligible variance in the profiles. In Figure 3.14 is a graphical representation of the amount of angles versus the computation time. From the profile plot it is clear that the effects of angle amount results in negligible changes to the profile, while linearly increasing in computation time as the amount of angles increase. As a result of these simulations it was determined that simulation only needed to be run with a minimum amount of angles.

(a) MCNP radiography image of an aluminum step block with a detector resolution of 578x726

(b) ADVANTG radiography image of an aluminum step block with a detector resolution of 578x726

Figure 3.11. Comparison of aluminum step block imaging in ADVANTG and MCNP for a detector resolution of 578x726

3.4.4. MCNP Particle History Impact. During the research as the MCNP FMESH got more fine the statistics of the detector intensity at each pixel started to decline. AS such to increase the image quality the number of particle histories increased. The effects of the amount of particles simulated compared to image quality and computation time was investigated further. It was already known that the amount of particle histories affected the computational time, however the effect of the image quality compared to the run time was not. The images were post-processed and are shown as contour plots in Appendix E. The comparison figures show that increasing the particle histories increases the image quality.

Table 3.2. The amount of particle histories and the effect of run times in MCNP.

Particle Histories	Time
$1E^{+4}$	0.03 minutes
$1E^{+6}$	0.07 minutes
$1E^{+9}$	42.17 minutes
$5E^{+9}$	212.00 minutes
$1E^{+10}$	427.10 minutes

Figure 3.12. Intensity profiles of an aluminum step block for MCNP and ADVANTG with a detector resolution of 578x726.

The error associated with $1E^{+10}$ particles is approximately 2%, which is acceptable error in the mesh tally. $5E^{+9}$ had error over 4% which is more than desired. So for the preformed simulations the particle histories used were $1E^{+10}$.

3.4.5. Limitation in ADVANTG. Two major limitations in ADVANTG were found that affected simulations, RAM limitations and processor thread limitations. RAM limitations directly correlate to the meshing size used which represents the desired resolution. AS the simulations were preformed reaching the realistic resolution of 578x726 required approximately 117GB of RAM. The RAM limit for the computer used was 128GB, the RAM alone was approximately $1000 needed to run the 578x726 resolution simulation. This was one of the major limitations found during the research. The other limitation was suspected to be a bug in the code. At a reasonably large mesh size ADVANTG could no longer run on a single CPU core. This limitation required a change in the OS from Windows 10 to Ubuntu 14.04 midway through the research. The Windows specific executable was

Figure 3.13. Intensity profiles at varying angles for the multi material ADVANTG simulations without flat field correction.

not compiled with MPI(Message Passing Interface) for use with multiple threads. This limitation was solved by switching to Linux where the code was compiled wit MPI and could be run using multiple threads.

3.5. COMPUTER AIDED DESIGN IMPORTATION

The importation of 3-D CAD models was achieved, the end result however was rather complicated. The importation mode failed to use macrobodies of any kind resulting in a MCNP input file that was complicated and difficult to navigate. After slight modifications and comparison to the original hand coded MCNP input file, it was possible to decipher each surface and cell.

3.5.1. CAD White Image Simulation. For these simulations the CAD input files were run in ADVANTG only as the MCNP results would be similar, and for this specific simulation the end goal was CAD importation into ADVANTG. The CAD model was based off of the Benchtop CT system models using 578x726 pixels. From the figures it is clear that for the white radiography image the CAD model and the Hand created input file are

Figure 3.14. Graphical representation of the effects of angle amount versus computation time in ADVANTG.

identical. The CAD imported file completed in 2362.5 seconds while the hand coded file completed in 2591.1 seconds. The CAD imported file completed 3.81 minutes faster then the hand coded file.

3.5.2. CAD Multi Material Imaging. The next simulation was the mulit material blocks everything was kept the same except that one input file was created by hand while the other used the CAD importation. Again from the simulation results it can be concluded that for the multi material scenario the CAD imported file and the hand created file are identical. The CAD imported file completed in 2573.9 seconds while the hand created file completed in 2580.9 seconds. The CAD file completed 7 seconds faster then the hand coded file which is negligible compared to the overall simulation time.

3.5.3. CAD Aluminum Step Block Imaging. The simulation results for the CAD imported file and the hand created file for the aluminum step block are identical. Again the simulations show that the CAD imported file yields the same radiography image. The run time for the CAD imported file was 2411.4 seconds and the run time for the hand

(a) A white radiography image from a hand created file.

(b) A white radiography image from a CAD imported file.

Figure 3.15. Comparison of Hand coded versus CAD imported input files for an ADVANTG white radiography image.

created file was 2408.0 seconds. The differences in run time between each method were negligible. From the combined results, using CAD importation is a viable option instead of hand created files for ADVANTG simulated radiography images.

3.5.4. Restrictions and Limitations. While the results showed that using a CAD imported file yields the same results it should be noted that some limitations exist in regards to importing a CAD file. The first limitation was the .SAT file type was the only extension accepted by VisEd. Not only that but only .SAT versions 4, 7, 8, 11, and 14 were accepted. Also because of limitations in MCNP no splines could be used in the CAD model. Another limitation that was encountered was model complexity limitations. Figure 3.21a3.21b shows an example of an overly complex model. To avoid this breaking the model up into more simplistic shapes was necessary. Beyond the limitations in the creation of the CAD model the importation output was also a limitation. Shown in Appendix D, the CAD model input file generated a much larger file than the hand created file. Not only this, but also some surfaces were generated with unrealistic parameters. While these unrealistic parameters had no affect on the output image, it did make understanding the geometry confusing.

Figure 3.16. ADVANTG profiles of CAD imported and hand coded input files for a white radiography image.

(a) Multi material radiography image for a hand created file.

(b) Multi material radiography image for a CAD imported file.

Figure 3.17. ADVANTG profiles of CAD imported and hand coded input files for a multi material radiography image.

Figure 3.18. Comparison of Hand coded versus CAD imported input files for an ADVANTG multi material radiography image.

(a) Aluminum step block radiography image for a hand coded file.

(b) Aluminum step block radiography image for a CAD imported file.

Figure 3.19. ADVANTG profiles of CAD imported and hand coded input files for a aluminum step block radiography image.

Figure 3.20. Comparison of Hand coded versus CAD imported input files for an ADVANTG aluminum step block radiography image.

(a) An example of an overly complex CAD model. A realistic model of the lead collimator.

(b) An example of a simplistic CAD model. A simplified model of the lead collimator.

Figure 3.21. Comparison of an overly complex CAD model and a CAD model that can be used for importation.

4. CONCLUSIONS

4.1. QUALITY VS TIME

As expected the ADVANTG deterministic code ran in a shorter period of time then the MCNP stochastic code. However the quality of the images generated by the deterministic code was unexpected. In the verification simulation of the isotropic point source, MCNP was expect to have less error than the simulation result showed, this was still within the margins of error. ADVANTG having a result closer to the theoretical values was unexpected, however. The area source model was another result that was unexpected. The MCNP model was as expected, the ADVANTG code was not. The ray effects resulted in ADVANTG not producing realistic results and forced the model to change to a simulated point source cone beam. It may be possible to use an area source in ADVANTG by setting a parameter to change the area source into a point source. For this simulation the cone beam assumption was close enough to the realistic model without the ray effects from a localized source. For the next set of simulations the ADVANTG simulations continued to take less computational time. Both profiles from ADVANTG and MCNP were acceptable and closely followed the expected profile. It was interesting to find that in the MCNP models as the simulated pixel amount increased the accuracy of the profiles decreased. This was a reasonable result as the particle tracks were expected to increase in error as the FMESH intervals increased. The last set of ADVANTG and MCNP comparison simulations continued to validate that ADVANTG would take less computational time than MCNP. ADVANTG was found to take approximately 10 times less time to complete than MCNP in a realistic radiography simulation. The ADVANTG image quality also steadily increased as the pixel amount increase where MCNP resulted in a slight decrease using the same amount of particle histories.

4.2. CAD IMPORTATION VS HAND CREATION

For the CAD importation models it is safe to conclude that from the results it will produce the same image as a hand created model with no impact in run time. While for simplistic models such as the multi material blocks model creating the input file by hand actually took less time to construct than creating a CAD model and adding the materials and other data cards. However for a complex model even with the limitations of importation, using the CAD model importation method could be a viable option. It should be noted that having a full understanding of the model is necessary as the importation can result in some unrealistic surfaces.

4.3. CODE VIABILITY

Compiling all results it is possible to conclude that ADVANTG is a viable option for creating synthetic radiography images. ADVANTG was shown to consistently complete in a shorter period of time than MCNP while generating higher quality images. A few limitations of ADVANTG although may pose issues. The first limitation is access to a system with a considerable amount of RAM. In the case of the realistic simulations 128GB of RAM was necessary. The second major limitation is that ADVANTG requires both the MCNP code and knowledge of MCNP input file creation to run. While in many situations this may not be an issue it still is a limiting factor that other deterministic codes may not have. Overall using ADVANTG to generate synthetic radiography images is a completely viable option in place of MCNP.

4.4. FUTURE WORK

While the results show that ADVANTG is a viable option as a replacement for MCNP to generated synthetic radiography images, the research in no way investigated all possible situations and scenarios. The first situation that was investigated but not full tested

was using multiple point sources in place of an area source. In Figure 4.1 it is possible to see that it was completely possible and generated comparable results to the single source simulations. Time limitations prevented further investigation. Figure 4.1 is a radiography image of the multi material simulation using 5 point sources to represent a 1mm x 1mm area source. Another situation could be using CAD models to simulate complex object

Figure 4.1. A 203x255 resolution radiography image of multi material blocks using 5 point sources.

images. Radiography images of objects within objects with varying densities, thicknesses and materials were not investigated.The effects of scattering and multiple beam energies were also not investigated. One final work that could be preformed is code optimization. Increasing the angles were shown to have little to no impact on the image quality. Lowering the amount of angles and the expansion order was not investigated. It is completely possible that with code optimization the computational time in ADVANTG could be reduced even further. Optimizing the code could also lead to less required RAM overhead as well.

APPENDIX A

DR. HYOUNG K. LEE'S BENCHTOP CT

BENCHTOP CT

       The figure below is the Benchtop CT used in the models, comprised of Source-Ray SourceBlock x-ray tube, 1ft x 1ft lead collimator, rotational stage (omitted from the simulations), and a Rayence CMOS flat panel detector.

APPENDIX B

MCNP INPUT FILE EXAMPLE

EXAMPLE MCNP CODE

Appendix 2 is an example MCNP code for 578x726 pixels of the white image Benchtop CT model.

```
C ================================ CELLS
  ================================
1     3   −11.35      −1 2              IMP:P=1   VOL=1114.316409
      $ COLUMNATOR
2     2   −0.001205  −2                IMP:P=1   VOL=9.465895694
      $ APERTURE
10    1   −7.44       −10              IMP:P=1   VOL=567.0757776
      $ DETECTOR
90    2   −0.001205  −90 1 2 10        IMP:P=1
                         $ VOLUME
100   0               90               IMP:P=0
                    $ KILL PARTICLES


C ================================ SURFACES
  ================================
C # RPP Xmin     Xmax     Ymin     Ymax       Zmin       Zmax
C  P.S.        0.01             15.31                   15.31
              $ POINT SOURCE
1   RPP   10.01   11.21    0.01    30.61     0.01     30.61
       $ COLLIMATOR
2   RPP   10.01   11.21   15.31   17.8151   12.7176
      15.8665   $ APERTURE
```

```
10 RPP    55.01    58.32    15.31    26.9524    3.1369
     17.8649    $ DETECTOR
90 RPP    0    58.33    0    30.62    0    30.62
        $ BOUNDS


C ------------------------------- MATERIALS

    --------------------------------

M1    8000.04P    0.084527    $ Gd2O2S  p = -7.44
 16000.04P    0.084704
 64000.04P    0.830769
M2    6000.04P    0.000150    $ AIR    p = -0.001205
 7000.04P    0.784431
 8000.04P    0.210748
 18000.04P    0.004671
M3    82000.04P    1    $ LEAD
C ----------------------------- SOURCE TERM

    --------------------------------

MODE P
SDEF PAR=2  X=0.01 Y=15.4 Z=15.31 VEC 1 0 0  DIR=D1 ERG=D2
SI1  H  0.9239    1.0
SP1    0.0    1.0
SI2 H 0    0.012    0.013    0.014    0.015    0.016    0.017
   0.018    0.019 &
0.02    0.021    0.022    0.023    0.024    0.025    0.026    0.027
     0.028 &
0.029    0.03    0.031    0.032    0.033    0.034    0.035    0.036
     0.037 &
```

0.038   0.039   0.04   0.041   0.042   0.043   0.044   0.045
        0.046 &

0.047   0.048   0.049   0.05   0.051   0.052   0.053   0.054
        0.055 &

0.056   0.057   0.058   0.059   0.06   0.061   0.062   0.063
        0.064 &

0.065   0.066   0.067   0.068   0.069   0.07   0.071   0.072
        0.073 &

0.074   0.075   0.076   0.077   0.078   0.079   0.08   0.081
        0.082 &

0.083   0.084   0.085   0.086   0.087   0.088   0.089   0.09
        0.091 &

0.092   0.093   0.094   0.095   0.096   0.097   0.098   0.099
        0.1   &

0.101   0.102   0.103   0.104   0.105   0.106   0.107   0.108
        0.109 &

0.11   0.111   0.112   0.113   0.114   0.115   0.116   0.117
        0.118 &

0.119   0.12

SP2 D 0   9.8732E-10 3.42979E-08 4.9972E-07 3.9548E-06
     1.99682E-05 7.02797E-05

0.00019141 0.000429918 0.000829093 0.001412351 0.002206809
     0.003176474

0.004318781 0.005549613 0.006866632 0.008166442 0.009540632
     0.010755399

0.011919467 0.012975658 0.013938599 0.014780197 0.015533148
     0.016145329

0.016647232 0.017054412 0.017375087 0.01759396 0.017745504
0.017824945

0.017844567 0.017807876 0.017732711 0.017592865 0.017439907
0.017239668

0.017028595 0.016781587 0.016519275 0.016244878 0.015938512
0.015646792

0.015335541 0.015033511 0.01470463 0.014384186 0.044300911
0.066666592

0.013427078 0.013105407 0.01278255 0.012465502 0.012158364
0.011843912

0.011539016 0.029277692 0.010937255 0.015382388 0.009715078
0.009464643

0.009228099 0.008995258 0.008761721 0.008533957 0.008302605
0.008079535

0.007856031 0.007636545 0.007419503 0.007204305 0.00699703
0.00678768

0.006584825 0.006379394 0.006180289 0.005985803 0.00579076
0.005601096

0.005411734 0.0052259 0.005043399 0.004862052 0.004684879
0.004508656

0.004335878 0.004162558 0.003993989 0.003826355 0.00366023
0.003497803

0.003332445 0.003171602 0.00301074 0.002850509 0.002692813
0.002532292

0.002376417 0.002215548 0.002058341 0.001899763 0.001739106
0.001579978

```
0.001403688  0.001233105  0.001063912  0.000897004  0.000664478
   0.000327068  0

FMESH4:P  GEOM=xyz        ORIGIN=55.01    15.31    3.1369
imesh=55.91           iints=1
jmesh=26.9524      jints=578
kmesh=17.8649      kints=726
NPS  1e10
PRDMP  1e10  1e10
 print
```

APPENDIX C

ADVANTG INPUT FILE EXAMPLE

EXAMPLE ADVANTG CODE

Appendix 3 is an example ADVANTG code for 578x726 pixels of the white image Benchtop CT model.

```
method                          dx


mcnp_input                      System.INP
outputs                          silo


mcnp_tallies                    4


mcnp_material_names     1     Detector
2     STPAir
3     Lead


anisn_library                   200n47g



denovo_x_blocks                 4
denovo_y_blocks                 3


denovo_quadrature               qr
denovo_pn_order                 3
denovo_quad_num_azi             4
denovo_quad_num_polar           4


dx_forward                                                  True
```

denovo_first_group   239

mesh_x   0   10.01   11.21   55.01   55.91
          58.33
mesh_x_ints   8   2   66   1
          1

mesh_y   15.31   26.9524
mesh_y_ints   578

mesh_z   3.1369   17.8649
mesh_z_ints   726

APPENDIX D

CAD INPUT FILE COMPARED TO HAND CREATED INPUT FILE

BENCHTOP CT

Appendix 4 shows the comparison between a hand created input file and an input file created by importing a CAD file.

```
Hand Coded
C ============================== CELLS ==============================
1    6 -11.35     -1 2              IMP:P=1  VOL=1488.090842  $ COLUMNATOR
2    2 -0.001205 -2                 IMP:P=1  VOL=10.08515798  $ APERTURE
10   1 -7.44      -10               IMP:P=1  VOL=567.0757776  $ DETECTOR
C 20 6 -11.35     -20               IMP:P=1  VOL=8.0          $ LEAD BLOCK
C 30 5 -2.699     -30               IMP:P=1  VOL=8.0          $ ALUMINUM BLOCK
90   2 -0.001205 -90 1 2 10         IMP:P=1                   $ VOLUME
100  0            90                IMP:P=0                   $ KILL PARTICLES
C ============================== SURFACES ==============================
C # RPP  Xmin    Xmax    Ymin    Ymax      Zmin     Zmax
C  P.S.     0.01          15.31           15.31         $ POINT SOURCE
1  RPP   10.01   11.61   0.01    30.61     0.01     30.61   $ COLLIMATOR
2  RPP   10.01   11.61   15.31   17.7651   12.7426  15.8165 $ APERTURE
10 RPP   55.01   58.32   15.31   26.9524   3.1369   17.8649 $ DETECTOR
90 RPP    0      58.33    0      30.62     0        30.62   $ BOUNDS
```

```
MCNPX Visual Editor Version X_24E
1     2 -0.001205   (-1 -2 -3 -4 -5 -6 )(7 :8 :9 :10 :11 :12 ) &
                    (7 :8 :9 :16 :17 :-11 )(7 :8 :9 :10 :23 :-17 ) &
                    (-11 :26 :17 :-16 :9:7 ) &
                    (7 :-26 :9 :10 :17 :-11 )(37 :38 :39 :-16 :41 :42 ) IMP:P=1
2     6 -11.35     (-7 -8 -9 -10 -11 -12 ) IMP:P=1
3     6 -11.35     (-7 -8 -9 -16 -17 11 ) IMP:P=1
4     6 -11.35     (-7 -8 -9 -10 -23 17 ) IMP:P=1
5     2 -0.001205 (11 -26 -17 16 -9 -7 ) IMP:P=1
6     6 -11.35     (-7 26 -9 -10 -17 11 ) IMP:P=1
7     1 -7.44      (-37 -38 -39 16 -41 -42 ) IMP:P=1
8     0            (1 :2 :3 :4 :5 :6 ) IMP:P=0

1       p -1 0 0 0
2       p 0 -1 0 0
3       p 1 0 0 58.33
4       p 0 1 0 30.62
5       p 0 0 1 30.62
6       p 0 0 -1 0
7       p -1 0 0 -10.01
8       p 0 -1 0 -0.01
9       p 1 0 0 11.61
10      p 0 1 0 30.61
11      p 0 0 1 12.7426
12      p 0 0 -1 -0.0099999999999989
13      p -1 0 0 -10.01
14      p 0 -1 0 -0.01
15      p 1 0 0 11.61
16      p 0 1 0 15.31
17      p 0 0 1 15.8165
18      p 0 0 -1 -12.7426
19      p -1 0 0 -10.01
20      p 0 -1 0 -0.01
21      p 1 0 0 11.61
22      p 0 1 0 30.61
23      p 0 0 1 30.61
24      p 0 0 -1 -15.8165
25      p 0 0 -1 -12.7426
26      p 0 1 0 17.7651
27      p 0 0 1 15.8165
28      p 0 -1 0 -15.31
29      p 1 0 0 11.61
30      p -1 0 0 -10.01
31      p -1 0 0 -10.01
32      p 0 -1 0 -17.7651
33      p 1 0 0 11.61
34      p 0 1 0 30.61
35      p 0 0 1 15.8165
36      p 0 0 -1 -12.7426
37      p 1 0 0 58.32
38      p 0 1 0 26.9524
39      p -1 0 0 -55.01
40      p 0 -1 0 -15.31
41      p 0 0 1 17.8649
42      p 0 0 -1 -3.1369
```

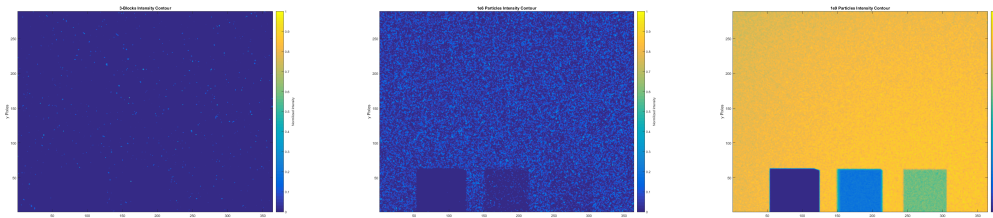(a) Hand coded input file for a white image, cells and surfaces only.

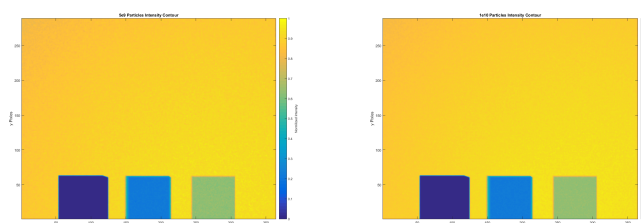(b) CAD imported input file for a white image, cells and surfaces only.

APPENDIX E

MCNP PARTICLE HISTORY CONTOUR PLOTS

MCNP PARTICLE HISTORY CONTOUR PLOTS

Appendix 5 shows the impact of the particle histories in MCNP for $1E^{+4}$, $1E^{+6}$, $1E^{+9}$, $5E^{+9}$, and $1E^{+10}$ particles.

(a) MCNP radiography image of multi material blocks with $1E^{+4}$ particles.

(b) MCNP radiography image of multi material blocks with $1E^{+6}$ particles.

(c) MCNP radiography image of multi material blocks with $1E^{+9}$ particles.

(d) MCNP radiography image of multi material blocks with $5E^{+9}$ particles.

(e) MCNP radiography image of multi material blocks with $1E^{+10}$ particles.

REFERENCES

T.M. Evans. *Denovo Methods Manual*. Oak Ridge National Laboratory, Oak Ridge, TN, 5.4 edition, July 2012.

Anthony Brinton Wolbarst. *Physics of Radiology*. Medical Physics Publishing, Madison, Wisconsin, 2012.

X-5 Monte Carlo Team. *MCNP-A General N-Particle Transport Code, Version 5*. Los Alamos National Laboratory, volume i: overview and theory edition, April 2003.

E.E. Lewis and Jr. W.F. Miller. *Computational Methods of Neutron Transport*. American Nuclear Society, Inc., La Grange Park, IL, 1993.

S.W. Mosher, S.R. Johnson, A.M. Bevill, A.M. Ibrahim, C.R. Daily, T.M. Evans, J.C. Wagner, J.O. Johnson, and R.E. Grove. *ADVANTG-An Automated Variance Reduction Parameter Generator*. Oak Ridge National Laboratory, Oak Ridge, TN, August 2015.

W.A. Rhoades and R.L. Childs. The dort two-dimensional discrete ordinates transport code. Abstract, Oak Ridge National Laboratory, Oak Ridge, TN, 1987.

W.A. Rhoades and R.L. Childs. A three-dimensional discrete ordinates neutron/photon transport code. Abstract, Oak Ridge National Laboratory, Oak Ridge, TN, 1990.

S. Johnson, T. Evans, G. Davidson, S. Hamilton, and T. Pandya. *Exnihilo Documentation*. Oak Ridge National Laboratory, Oak Ridge, TN, 5.4 edition, July 2015.

Gavin G. Poludniowski and Philip M. Evans. Calculation of x-ray spectra emerging from an x-ray tube. part i. electron penetration characteristics in x-ray targets. *Medical Physics*, 34(6):2164–2174, 2007. ISSN 2473-4209. URL http://dx.doi.org/10.1118/1.2734725.

Gavin G. Poludniowski. Calculation of x-ray spectra emerging from an x-ray tube. part ii. x-ray production and filtration in x-ray targets. *Medical Physics*, 34(6):2175–2186, 2007. ISSN 2473-4209. URL `http://dx.doi.org/10.1118/1.2734726`.

G Poludniowski, G Landry, F DeBlois, P M Evans, and F Verhaegen. Spekcalc : a program to calculate photon spectra from tungsten anode x-ray tubes. *Physics in Medicine and Biology*, 54(19):N433, 2009. URL `http://stacks.iop.org/0031-9155/54/i=19/a=N01`.

J.H. Hubbell and S.M. Seltzer. Tables of x-ray mass attenuation coefficients and mass energy-absorption coefficients, 2004. URL `http://physics.nist.gov/xaamd`.

Model SB-160-4K-BW. Source-Ray, Inc., Ronkonkoma, NY.

Rayence. *CMOS Flat Panel Sensor*. Korea.

Hyoung-Koo Lee, Do-Il Kim, Sung-Hyeon Kim, Dae-Sop Park, Bo-Young Choe, and Tae-Suk Suh. An iterative method for flat-field correction of digital radiography when detector is at any position. volume 5745, pages 1025–1029, 2005. URL `http://dx.doi.org/10.1117/12.595394`.

VITA

Andrew Albert Bingham, born 1992. Received a Bachelors of Science in Nuclear Engineering from the University of Science and Technology in May 2015 and went on to receive a Master of Science in Nuclear Engineering from Missouri University of Science and Technology in May 2017.